ACS APPLIED BIO MATERIALS

www.acsabm.org

Article

Fast and Effective Deactivation of Human Coronavirus with Copper Oxide Suspensions

Mutalifu Abulikemu, Edward P. Booker, Bita E.A. Tabrizi, and Ghassan E. Jabbour*

Cite This: https://doi.org/10.1021/acsabm.2c00229

Read Online

ACCESS | Metrics & More | Article Recommendations | Supporting Information

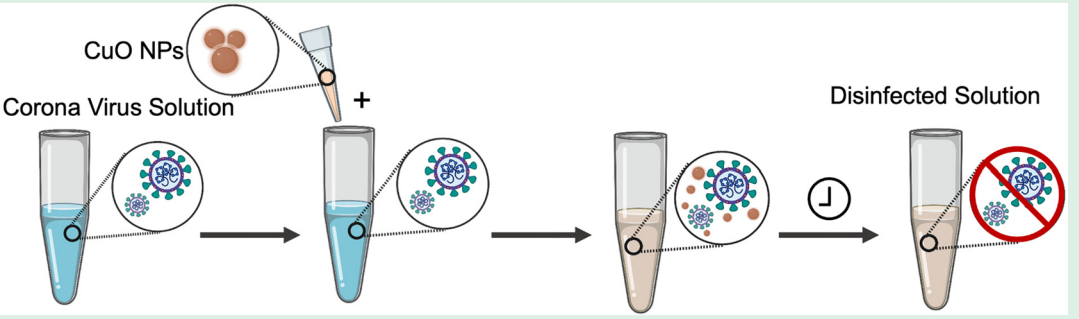

ABSTRACT: The COVID-19 pandemic has demonstrated the need for versatile and robust countermeasures against viral threats. A wide range of viruses, including SARS-CoV-2, the virus that causes COVID-19, can be deactivated by metal and metal-oxide surface coatings. However, such coatings are expensive and cannot easily be retrofitted to existing infrastructure. Low-cost materials to halt the propagation of a variety of viruses must be produced with minimal quantities of expensive precursors. In this regard, we show that commercially available copper oxide nanoparticle suspensions can deactivate more than 99.55% of the human coronavirus 229E in 30 min, confirming the particles' efficiency as a fast antiviral material.

KEYWORDS: *CuO, nanoparticles, human coronavirus, COVID-19, virus, face mask*

INTRODUCTION

The ongoing pandemic has demonstrated the difficulty in stopping the spread of SARS-CoV-2 virus with traditional methods. On the other hand, developing new vaccines to deal effectively with the virus and its mutations can take years.[1] The SARS-CoV-2 virus has permanently changed global society and caused more than 5.2 million deaths according to the World Health Organization (WHO).[2] The established pharmaceutical development procedures are being questioned to help hasten the introduction of new highly reliable vaccines.[3] Many governments' isolation policies are disrupting people's daily lives,[4] impacting education, harming businesses,[5] and damaging economies,[6] particularly in service-oriented countries. We need novel, broad-spectrum viricides that can destroy viruses on contact within a short amount of time and improve personal protection, especially medical professionals.

The SARS-CoV-2 virus is a member of the Coronaviridae family of viruses, which includes SARS-CoV, H5N1 influenza A, HCoV-299E, and H1N1 viruses.[7] These viruses, harboring the largest genome of 26−32 kilobases among RNA viruses, were termed "CoVs" because of their crownlike morphology under an electron microscope.[8,9] Because of its similar structure to SARS-CoV-2, the human coronavirus (HCoV-299E) strain has frequently been utilized as a surrogate virus for SARS-CoV-2, allowing lower-biosafety-level facilities to work on SARS-CoV-2 treatments.[10] Many of the most severe virus outbreaks in recent decades have been caused by this family of viruses, demonstrating the need for innovative approaches to dealing with them.[11] Prevention is preferable to treatment, which motivates efforts to protect ourselves from them, both through prophylaxis and avoiding initial encounter with the virus.[12,13] This has motivated our work on finding practical and low-cost antiviral materials.

Metal and metal oxide layers can deactivate and kill viruses on surfaces; however the rates of deactivation vary, and the processes for virus termination are still being uncovered. The mechanism proposed for this deactivation is that the surface chemically reacts with the virus, leading to its destruction.[14−16] Vacuum-deposited metal layers are somewhat expensive and do not fit perfectly to the geometrical form of many surfaces. Furthermore, metal particle cold-spray procedures in inert conditions cannot result in deeper penetration of such particles into porous surfaces, reducing the coating's operational disinfectivity and mechanical stability. An in situ growth process of metallic particles must be used to achieve better infiltration of the coating in a porous medium.[17]

Received: March 14, 2022
Accepted: June 7, 2022

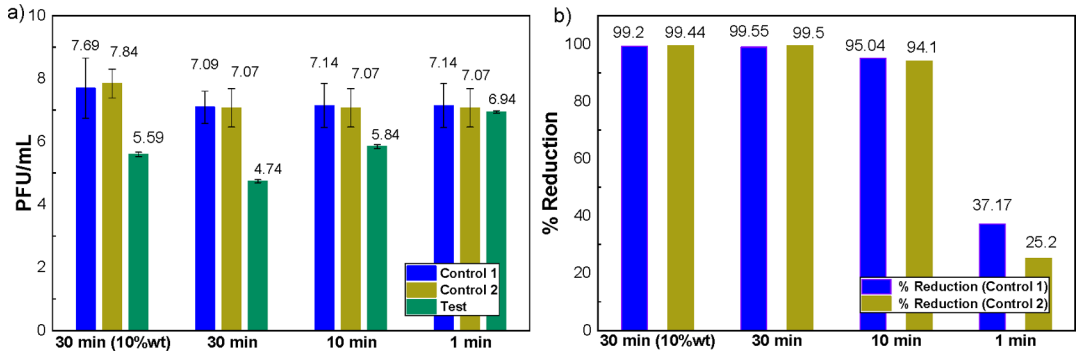

Figure 1. Results of assays measuring antiviral effects of CuO NPs. (a) Log geometric mean of the triplicated HCov-229E infectivity test after introducing nanoparticles and remaining in contact for three different intervals of 1, 10, and 30 min (green) before infecting cells. Assays with no NP contact were used as control 1 (blue), and assays where the samples were exposed to NPs as they were diluted as control 2 (chartreuse yellow). (b) Percent reduction graphs from assays of the CuO NP viricidal efficiency on HCoV-229E. This was compared to the same virus pool with no CuO NP contact (control 1, blue), or the same virus pool exposed to CuO NPs as the samples were diluted (control 2, chartreuse yellow).

Table 1. Details of Viricidal Assay of HCoV-229E[a]

Experiment	Test	SD	LC1	SD	LR1	SD	%R1	SD	LC2	SD	LR2	SD	%R2	SD
CuO 10% (30 mins)	5.59	0.07	7.69	0.96	2.1	0.11	99.2	0.2	7.84	0.46	2.25	0.11	99.44	7.9
CuO 20%(30 mins)	4.74	0.05	7.09	0.51	2.35	0.08	99.55	0.5	7.07	0.61	2.33	0.08	99.5	8.37
CuO 20%(10 mins)	5.84	0.06	7.14	0.65	1.3	0.05	95.0	0.2	7.07	0.61	1.23	0.07	94.1	7.83
CuO 20%(1min)	6.94	0.04	7.14	0.65	0.2	0.08	37	0.15	7.07	0.61	0.13	0.08	25.2	7.92

[a]Test column stands for the ($\log_{10}$) PFUs measured when exposing the HCoV-229E virus to CuO NPs. SD is the standard deviation of the relevant measurement. The columns labeled LC1 and LC2 are the ($\log_{10}$) measured PFUs of control samples using method 1 and 2, respectively. LR1 and LR2 are the ($\log_{10}$) reduction in PFUs of the test results in comparison to LC1 and LC2, respectively. %R1 and %R2 are the percentage reduction of the tests calculated using controls from method 1 and 2, respectively. The %R and associated SD columns are highlighted in lavender-grey color for emphasis.

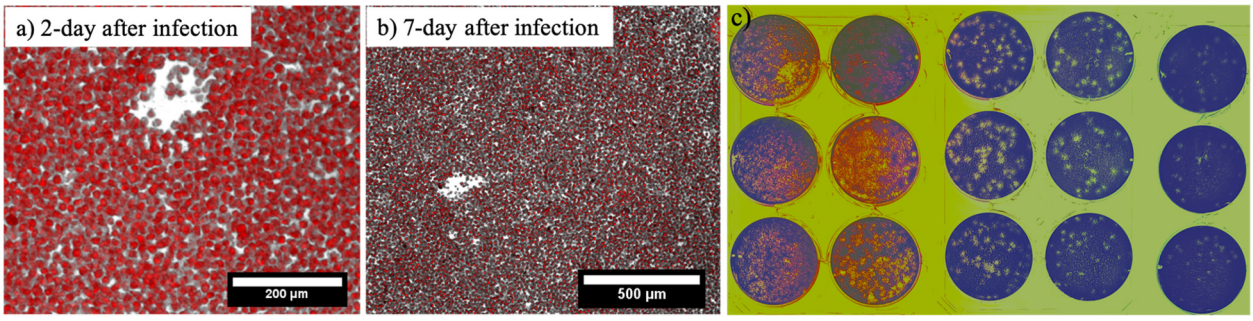

Figure 2. Microscope image showing plaques formed and how they were counted. (a, b) Plaque development captured by a fluorescence microscope using an object after 2 and 7 days of infecting the L-132 cell line with HCoV-229E, respectively. A mix of media, 2% FBS, 0.5% low melting agarose, and 0.03% neutral red was overlaid 2 days before the image was taken. Neutral red stains the viable cells, making them easily identifiable. (c) Images of the plaques formed in titrating HCoV-229E in L-132 cells. The infected cells were monitored by a microscope to define the time countable viral plaques clearly present. The counting of the plaques is challenged in the narrow time window after several days. The right time is when the surviving viruses have had the opportunity to make a visible plaque but have not diffused into another plaque. After presenting countable plaques, the cells were fixed by 10% formaldehyde and stained by 0.5% crystal violet. The titration of the virus was calculated using the following formula: [HCoV-229E] PFU/mL= (total number of plaques in the three wells with countable plaques/3) × (serial dilution factor) × (the sample dilution factor).

Nanomaterials are materials with at least one dimension having a length scale on the order of 1−1000 nm. These materials have properties that can be altered by controlling their size.[18] Such properties may include electronic bandgap,[19] plasmonic resonance,[20] and chemical potential.[21] Metal and metal oxide nanoparticles (NPs) have been shown to be effective against viruses.[22,23] Three models for how NPs can deactivate or halt viral infection are as follows: (1) metal ions are released from NPs and chemically react with virus proteins, destroying the virus;[24] (2) NPs can accumulate in key areas where the virus would attack the host, preventing it from gaining entry;[25] and (3) NPs can bind with the proteins coating the virus and as such prevent it from interacting with anything else other than the NPs.[16,26]

Because of their desirable efficacy, as well as their cheaper and easier manufacturing, copper-based NPs and cuprous oxide (Cu_2O) have gotten a lot of attention in the quest for widely available materials made of relatively abundant elements

https://doi.org/10.1021/acsabm.2c00229
ACS Appl. Bio Mater. XXXX, XXX, XXX−XXX

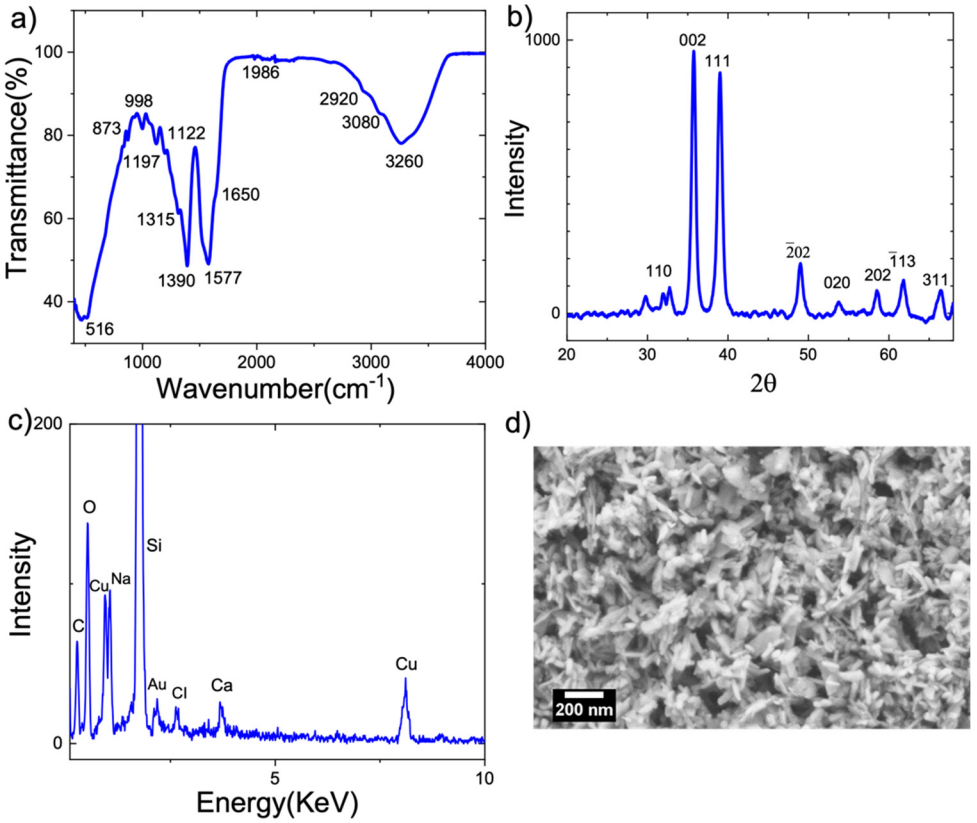

Figure 3. (a) FTIR of drop-cast NP films. The peaks consistent with the coordinating solvents are highlighted. Peaks at 872 and 516 cm^{-1} are consistent with Cu−OH bonds and Cu−O bonds, respectively. (b) XRD spectrum of drop-cast film of CuO NPs. Peaks are consistent with monoclinic CuO, and notable peaks are indicated with their Miller indices. (c) EDX spectrum of CuO NPs. Elements are annotated on the associated peaks. (d) SEM of the drop-cast CuO NPs as measured by us (scale bar 200 nm).

that are successful in deactivating communicable diseases.[27−29] Such materials were proven to deactivate the influenza virus and SARS-CoV-2.[30−34] In this communication, we show that commercially available aqueous suspensions of copper(II) oxide (CuO) NPs are able to effectively destroy a coronavirus. In fact, CuO NP suspensions kill more than 99.55% of coronavirus in less than half an hour, according to viral tests. To verify the integrity of our experimental results, we used two complementary control experiments to calculate the efficacy of our NPs solutions. We further analyzed the structure and makeup of the NPs using a variety of characterization methods. Our findings suggest that metal oxide NPs can be used as active viricides in a number of settings, including viricidal surfaces, fabrics, and solutions. We illustrate how these NPs may be easily included into personal protective equipment for active viricidal protection as an example of how this technology can be used.

RESULTS

We used two formulations of CuO NPs in our viricidal assays, the as-purchased CuO nanoparticles at 20 wt % in aqueous suspension, and a 10 wt % aqueous suspension (see Materials and Methods). Ten weight percent solutions of as-purchased CuO NPs were dosed with HCoV-229E and only after 30 min of exposure the sample was halted by dilution. After this, the number of plaque forming units (PFUs) was measured to determine the amount of virus that had been deactivated (see Materials and Methods). This test demonstrated a 2log reduction in plaque forming units compared to control experiments (Figure 1). This result prompted us to try the higher concentration of 20 wt % CuO NPs suspension. These experiments were repeated with three different exposure times of 1, 10, and 30 min, after which the exposure was halted by dilution. The results show that a 30 min exposure of HCoV-229E to 20 wt % CuO NPs causes a 2.35 log reduction in PFUs. The details of these experiments and their results are given in the Materials and Methods section and Table 1, respectively. A microscope image of plaques identified during these experiments is shown in Figure 2. The reduction in PFUs for each experiment was analyzed with respect to two different control samples. For control 1, we diluted the samples having no contact with NPs after the incubation times used in our experiments (1, 10, and 30 min) and then determined the number of PFUs. In the second method, we inoculated our control samples with NPs after the relevant incubation times (1, 10, and 30 min) and then immediately diluted them to be used for a plaque forming assay. The purpose of adding the NPs to the control is to ensure that the effect of NPs on the virus during dilution is taken into account. As can be seen from our results (Figure 1 and Table 1), the effect of NPs on the number of PFUs after dilution is not statistically significant, nor is there a general trend between the two control methods.

A Fourier transform infrared spectroscopy (FTIR) study (Figure 3a, details in Table S1) shows low energy peaks at 536 and 871 cm^{-1} indicative of Cu−O and Cu−O−H bonds, respectively.[35] The peaks associated with the organic component are given in Table S1. Analysis of the energy-dispersive X-ray spectroscopy (EDX) spectra (Figure 3c and

https://doi.org/10.1021/acsabm.2c00229
ACS Appl. Bio Mater. XXXX, XXX, XXX−XXX

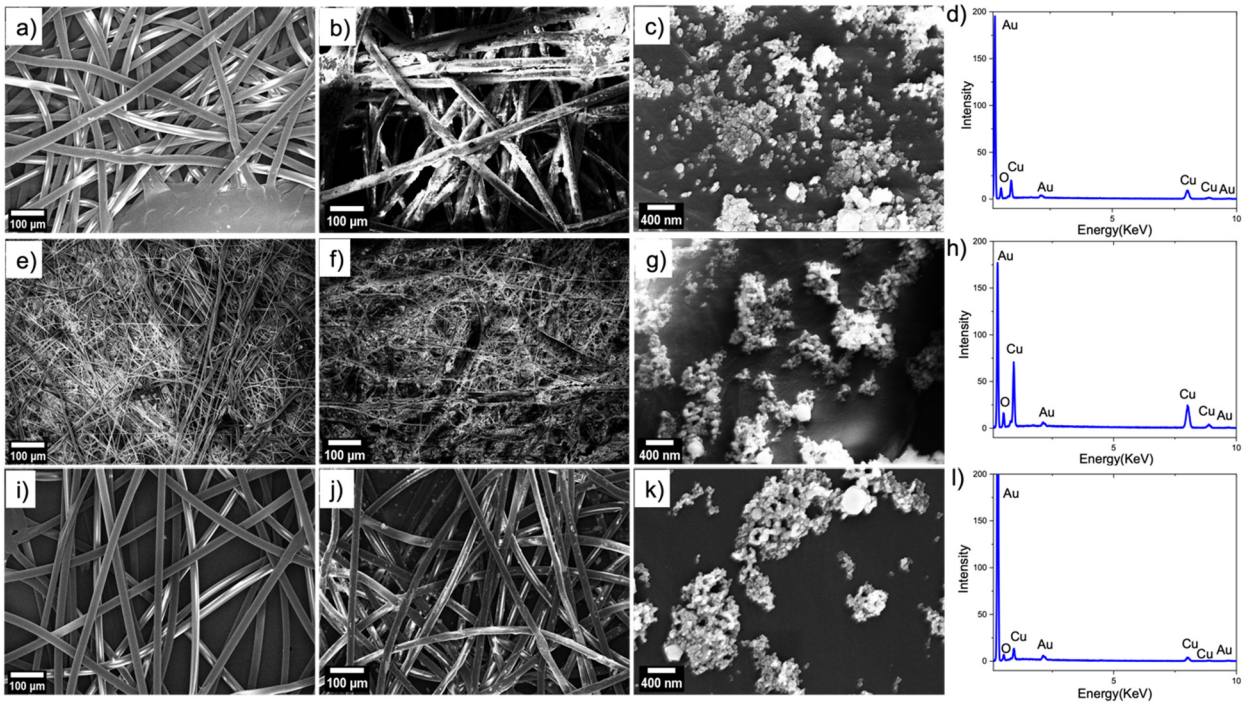

Figure 4. (a, e, and i) SEM images of the uncoated front, middle, and back layers of the surgical face mask, respectively. SEM images of the three different layers of the CuO NP-coated mask at two different magnifications: (b, c) the front layer, (f, g) the middle melt-blown layer, and (j, k) the back layer. (d, h, and l) EDX spectra of the CuO NP-coated front, middle, and back layers of mask indicate the presence of pure CuO with no contamination. The Au peak is caused by sputtering 5 nm Au on the mask to facilitate better SEM imaging.

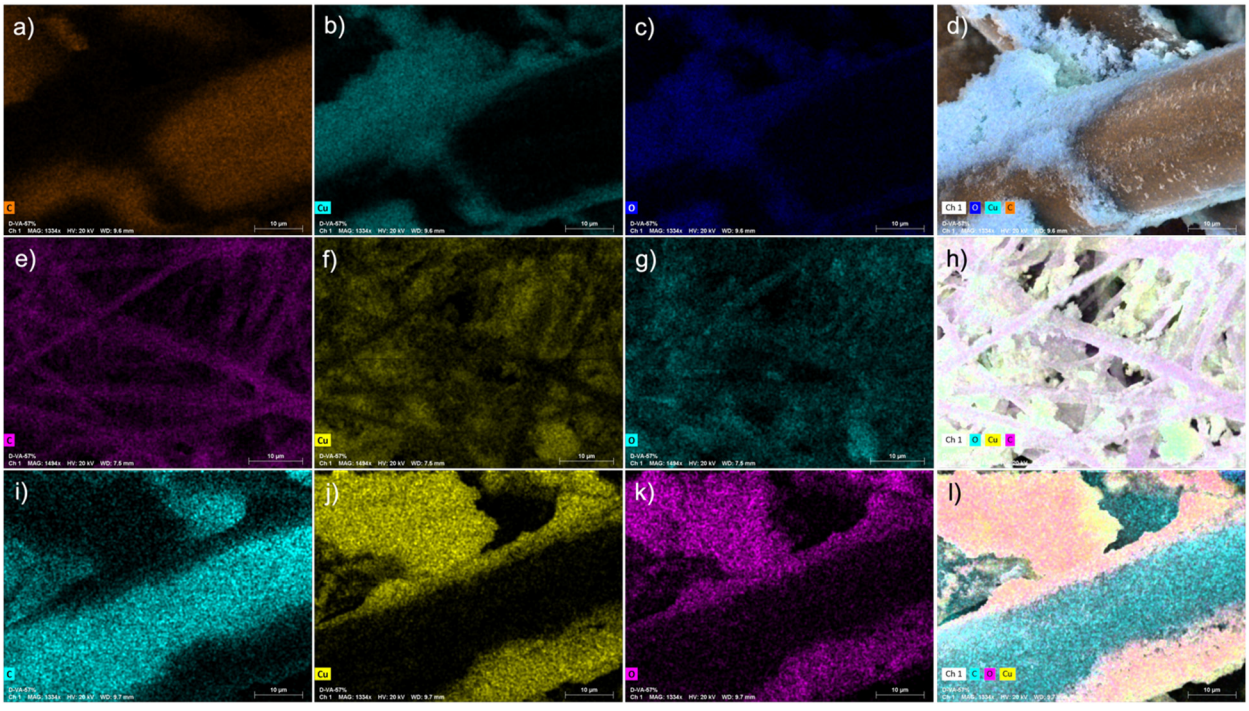

Figure 5. Elemental color mapping (EDX-SEM analysis) images of three layers of the CuO NP-coated surgical mask. (a–d) Front layer, (e–h) middle melt-blown layer, and (i–l) back layer.

Figure S3) indicates the presence of Cu, O, Si, Ca, Au, Cl, and Na. The presence of Na may suggest that a surfactant has been used to stabilize the particles in water or may be left over from the NP synthesis. Ca and Cl are listed as an impurity by the supplier, and Au was used in substrate preparation to prevent charging during SEM imaging. The crystal structure of these nanoparticles is demonstrated using X-ray diffraction (XRD) which shows that of CuO (Figure 3b), in agreement with the supplier's and published spectra (Figure S1a). Moreover, scanning electron microscopy (SEM) results show ∼200 nm long nanorods, with a cross-sectional diameter of ∼20 nm (Figure 3d and Figure S1b).

https://doi.org/10.1021/acsabm.2c00229
ACS Appl. Bio Mater. XXXX, XXX, XXX−XXX

We additionally prepared a prototype face mask impregnated with CuO NPs. This mask (Figure S2) was prepared by dip-coating a commercially available face mask into a solution of 20 wt % CuO NPs for 1 h and dried overnight. The SEM and elemental color mapping images of uncoated and coated layers of the mask are shown in Figures 4 and 5, respectively. This prototype's antiviral characteristics, stability, and safety for the human body when breathing and inhaling are currently being investigated.

DISCUSSION

CuO NPs can efficiently kill more than (99.55 ± 0.5)% of HCoV-229E virus within 30 min. These results are promising as it has been shown that the HCoV-229E virus behaves similarly to the SARS-CoV-2 virus responsible for the COVID-19 illness.[10] Indeed, with a small amount of optimization of the disinfectant suspension it is possible to develop a biologically compatible antiviral suspension based on abundant materials.

For both control methods, doubling the concentration of NPs decreases the final concentration of PFUs substantially, by approximately halving the remaining PFU count (Table 1). Although we do not currently have the data to determine the full relationship between concentration and kill rate, this is sufficient to show a promising trend. More research is needed to determine the exact relationship, which will shed light on the mechanisms by which NPs destroy viruses. Similarly, we have seen that the 20 wt % NP solution kills more than 95% of viruses in the first 10 min, and more than 99.55% in 30 min. A similar trend was seen for both control methods. Although the data are insufficient to draw any conclusions, we can observe that these solutions are quite quick to act. CuO NPs' viricidal mechanisms will be better understood with more time series data, which will aid in optimizing the NPs and their suspensions as a virucide effective against SARS-CoV-2.

The NP solutions used present no crystalline material other than monoclinic CuO as shown in the XRD spectrum (Figure 2c). This result alone is insufficient to suggest there are no other species that may kill the virus. The FTIR (Figure 2a) spectra we measured are very similar to the NPs synthesized by El-Kemary and co-workers, who did not use additional coordinating ligands.[35] The nanoparticles of El-Kemary were covered with a layer of acetate ions, which is consistent with the FTIR we measured. It is possible that these acetate ions facilitate binding of the virus with the nanoparticle unit, which effectively kills it, or that the CuO chemically reacts with the proteins coating the virus, which also leads to terminating it. As a result, an interaction between the NPs and the virus is concluded to deactivate or eliminate the virus. This is in line with Delogu and colleagues' findings, albeit more research is needed to fully understand the antiviral mechanism.[36] Judicially tailoring the coordinating ligands to the NPs could possibly allow for (1) enhanced NP binding with given viruses, (2) increased NP concentration to accelerate interactions with viruses, and (3) optimized composition to further improve the denaturing of virus proteins.[37] We intend to develop cost-effective materials that destroy viruses more quickly based on these findings.

Furthermore, the sodium ions (Na^+) in the CuO NP suspension may have a role in virus deactivation, but their concentrations are unlikely to be high enough to exhibit substantial antiviral activities in this setting. Because water is used to build the plaques in the first place, it is doubtful that the NP solvent, water, will eradicate the virus. CuO NPs have been shown to be cytotoxic to human cells in a variety of investigations, with toxicity varying depending on particle shape, size, surface functionalization, and time-dose interaction.[38,39] On the other hand, the results of the cytotoxicity of CuO microparticles (<5 μm) against A549 and HeLa S3 cells show that there is not any sign of cytotoxic effects on either cells after 24 h of incubation.[34,40] The median lethal dose (LD50) of cupric oxide for rats is 2500 mg/kg (oral) and 2000 mg/kg (dermal), with no signs of skin irritation or sensitization.[34,41] Moreover, some researchers have discovered that copper consumption varies by age group, and that there is a link between the amount of copper in the human body and certain diseases.[42] As a result, more research into the effects of CuO-coated PPEs on human health during ingestion and inhalation is required.

The high viricidal efficiencies found in this study prompted the development of active viricidal face masks, which are currently being studied for their viricidal efficacy. In this regard, Figures 4 and 5 show SEM and elemental color mapping images of the three different layers of one such mask, respectively. The images indicate that the CuO NPs penetrate all three layers of the mask, boosting virus disinfection rate. The EDX spectra are redrawn in Figure S4 for all three layers with the Au peak at 0.21KeV taken out. This assists in bringing forth the Cu peaks in all three layers of the coated mask. As expected, the data indicate that the intermediate melt blown layer absorbs more CuO NPs because of its large surface area.

CONCLUSIONS

We have demonstrated that CuO NPs can rapidly neutralize the HCoV-229E virus, a practical surrogate of the SARS-CoV-2 virus. The exact antiviral mechanism of CuO NPs was not investigated in this manuscript. However, the annihilation of the HCoV-229E virus is thought to be accelerated either by the virus attaching to the NPs' surface or by the nanoparticles denaturing the virus's surface proteins, thereby killing the virus because it can no longer enter a host cell and proliferate. These NPs will be suitable for self-disinfecting coatings and surfaces, sanitizing solutions that actively kill a broad-spectrum of viruses, as well as active antiviral personal protective equipment. Such solutions would provide long-lasting, active protection to frontline workers against many current and future viral threats. The potential for these NPs to be broad-spectrum antiviral defenses that are indifferent to virus' strain or structure is an exciting proposition that motivates further work.

MATERIALS AND METHODS

Materials. Copper oxide (CuO) NPs (99%, 40 nm) were purchased from US Research Nanomaterials (https://www.us-nano.com/inc/sdetail/222) fully dispersed in water at 20 wt %. Further dispersions were prepared by diluting the as-purchased suspension with appropriate volumes of deionized water.

Characterizations. Fourier transform infrared spectroscopy (FTIR): ~5 mL of 20 wt % concentrated CuO NPs were drop casted on a clean glass substrate and dried at 70 °C on a hot plate between each layer. FTIR was performed using Thermo Scientific NICOLET 6700. The as-prepared CuO solid film was mounted on FTIR, and the spectrum was obtained at wavenumbers 400−4000 nm.

Scanning Electron Microscopy (SEM). Two drops of 20 wt % concentrated CuO NPs were placed on clean silicon wafer and allowed to dry at room temperature overnight. SEM (Zeiss Gemini 500) was used to measure the morphological properties of CuO NPs.

https://doi.org/10.1021/acsabm.2c00229
ACS Appl. Bio Mater. XXXX, XXX, XXX−XXX

Simultaneously, EDX was measured to verify the integrity of commercial CuO NP composition.

X-ray Diffraction (XRD). A Rigaku Ultima IV diffractometer was used to acquire the XRD spectrum of the CuO NPs. XRD spectra were measured using CuKα radiation λ = 1.5406 Å with 2θ between 20 and 70° and a $\Delta\theta$ = 0.02°. Samples were prepared with drop casting ~5 mL of 20 wt % CuO NPs on a clean silicon wafer. The film was dried at 70 °C on a hot plate.

Virucidal Assay. For the virucidal experiments, the L-132 cell line (ATCC #CCL-5) originally derived from human embryonic lung tissue was used for propagation of the HCoV-229E (ATCC#VR-740). The cell line was primarily subcultured and grown in α-MEM media (GIBCO-BRL Cat # 41600-016) containing L-glutamine and 10% fetal bovine serum (FBS) in a T-75 cell culture flask. Afterward, 200 μL of virus stock having titration of one plaque per cell was added to the cultured L-132 cell monolayer and incubated for 1 h (at 35 °C and 5% CO_2). The media was then refreshed with α-MEM having 2% FBS while the incubation continued before the appearance of any cytopathic effects. Within 3 days, when the rounded up and detached cells were seen, the cell-virus suspension was pipetted out for harvesting the replicated virus. Then, a freeze−thawing cycle was carried out three times followed by centrifugation at 1000 × *g* for 10 min to purify the virus from the infected cell. An aliquot of the harvested virus pool was titrated by serial dilution for a plaque-forming assay to find the proper dilution of the virus pool that could be used in the virucidal activity test of the CuO NPs.

All testing procedures and the results were performed and reported according to ASTM E1153-03, Standard Test Method for Efficacy of Sanitizers Recommended for Inanimate Non-Food Contact Surfaces and CAN/CGSB-2.161-97, Assessment of Efficacy of Antimicrobial Agents for Use on Environmental Surfaces and Medical Devices. The stock HCoV-229E and two 10× dilutions were prepared in a soil load with a final concentration of 5% FBS.

Equal volumes (40 μL) of this virus suspension and CuO NPs were mixed and incubated for the planned contact time (1, 10, and 30 min), after which they were titrated into 10× serial dilution vials and subjected to plaque-forming assay.

In these tests, two types of controls were applied: (1) titrating the same virus pool without contacting the nanoparticles and (2) titrating the sample pool of the virus directly after mixing with the nanoparticles without incubation.

For the plaque-forming assay, 100 μL of the dilution of the test samples as well as controls replaced the media of the monolayer of L-132 cells cultured in six-well plates, followed by incubation of the plates at 35 °C in a 5% CO_2. After 1 h, the solution in each well was refreshed with 2 mL of medium containing 2% FBS and 0.5% low melting agarose. The second layer of agarose media, including 0.03% of neutral red (Sigma-Aldrich, Cat# N6264- 50 ML), was added on the fourth day of incubation. The neutral red stains eases the observation of the forming plaques through staining the live cells. Next step was fixing the cells by adding 10% buffered formalin, removing the media and finally, staining the cells with 0.5% crystal violate. After the plates were rinsed, the plaques became apparent, having a specific form that HCoV-229E causes. The geometric mean, the percent reduction, and the log reduction were calculated from counting the number of formed plaques. Our calculations were based on ASTM E1153-03, Standard Test Method for Efficacy of Sanitizers Recommended for Inanimate Non-Food Contact Surfaces.

■ ASSOCIATED CONTENT

Supporting Information

The Supporting Information is available free of charge at https://pubs.acs.org/doi/10.1021/acsabm.2c00229.

XRD of CuO NPs provided by the supplier and SEM images of CuO NPs; image of CuO-loaded active antiviral face mask prepared through dip-coating; SEM image used for EDX; EDX spectrum of the CuO NPs coated on the mask; table for assignment of FTIR peaks (PDF)

■ AUTHOR INFORMATION

Corresponding Author

Ghassan E. Jabbour − *School of Electrical Engineering and Computer Science, University of Ottawa, Ottawa, Ontarip K1N 6N5, Canada*; Email: gja@uottawa.ca

Authors

Mutalifu Abulikemu − *School of Electrical Engineering and Computer Science, University of Ottawa, Ottawa, Ontarip K1N 6N5, Canada*; orcid.org/0000-0002-8848-6804

Edward P. Booker − *School of Electrical Engineering and Computer Science, University of Ottawa, Ottawa, Ontarip K1N 6N5, Canada*

Bita E.A. Tabrizi − *School of Electrical Engineering and Computer Science, University of Ottawa, Ottawa, Ontarip K1N 6N5, Canada*; orcid.org/0000-0002-7812-1684

Complete contact information is available at: https://pubs.acs.org/10.1021/acsabm.2c00229

Notes

The authors declare no competing financial interest.

■ ACKNOWLEDGMENTS

We thank the Flow Cytometry and Robotic Facility at University of Ottawa for carrying out the virus assay test and analysis, as well as Dr. Shahrokh M. Ghobadloo for his helpful discussion of the virus assay test results during manuscript preparation. We also thank Hamed M. Mofarah for his assistance with SEM characterizations. G.E. Jabbour acknowledges the support of Canadian government through the Canada Research Chair (Tier 1) (award 950-231466) and NSERC Discovery Grant (award RGPIN-2020-06970).

■ REFERENCES

(1) Amanat, F.; Krammer, F. SARS-CoV-2 vaccines: status report. *Immunity* **2020**, *52*, 583−589.

(2) *WHO Coronavirus (COVID-19) Dashboard*. World Health Organization. https://covid19.who.int/, 2021 (accessed 2021-12-15).

(3) Caplan, A. L.; Bateman-House, A. The danger of DIY vaccines. *Science* **2020**, *369*, 1035.

(4) Rawat, D.; Dixit, V.; Gulati, S.; Gulati, S.; Gulati, A. Impact of COVID-19 outbreak on lifestyle behavior: A review of studies published in India. *Diabetes Metab. Syndr.: Clin. Res. Rev* **2021**, *15*, 331−336.

(5) De Oliveira Araújo, F. J.; de Lima, L. S. A.; Cidade, P. I. M.; Nobre, C. B.; Neto, M. L. R. Impact of Sars-Cov-2 and its reverberation in global higher education and mental health. *Psychiatry Res.* **2020**, *288*, 112977.

(6) Szmigiera, M. *Impact of the coronavirus pandemic on the global economy - Statistics & Facts*; Statista:nNew York, 2021. https://www.statista.com/topics/6139/covid-19-impact-on-the-global-economy/#dossierKeyfigures.

(7) Shereen, M. A.; Khan, S.; Kazmi, A.; Bashir, N.; Siddique, R. COVID-19 infection: Origin, transmission, and characteristics of human coronaviruses. *J. Adv. Res.* **2020**, *24*, 91−98.

(8) Yuan, Z. W.; Ye, S.; Yuen, K. S.; Fung, S. Y.; Chan, C. P.; Jin, D. Y. Zoonotic origins of human coronaviruses. Int. *J. Biol. Sci.* **2020**, *16*, 1686−1697.

(9) Chen, B.; Tian, E. K.; He, B.; Tian, L.; Han, R.; Wang, S.; Xiang, Q.; Zhang, S.; El Arnaout, T.; Cheng, W. Overview of lethal human coronaviruses. *Sig Transduct Target Ther* **2020**, *5*, 89.

(10) Signer, J.; Jonsdottir, H. R.; Albrich, W. C.; Strasser, M.; Zust, R.; Ryter, S.; Ackermann-Gaumann, R.; Lenz, N.; Siegrist, D.; Suter, A.; Schoop, R.; Engler, O. B. In vitro virucidal activity of Echinaforce®, an Echinacea purpurea preparation, against coronaviruses, including common cold coronavirus 229E and SARS-CoV-2. *Virol. J.* **2020**, *17*, 1−11.
(11) de Wit, E.; van Doremalen, N.; Falzarano, D.; Munster, V. J. SARS and MERS: recent insights into emerging coronaviruses. *Nat. Rev. Microbiol* **2016**, *14*, 523−534.
(12) Xinguang, C. Experiences of surveillance, influential factors, and prevention to end the global coronavirus disease 2019 (COVID-19) pandemic. *J. Glob. Health* **2021**, *5*, 1−3.
(13) Ullah, H.; Ullah, A.; Gul, A.; Mousavi, T.; Khan, M. W. Novel coronavirus 2019 (COVID-19) pandemic outbreak: A comprehensive review of the current literature. *Vacunas* **2021**, *22*, 106−113.
(14) Murray, J. P.; Laband, S. J. Degradation of poliovirus by adsorption on inorganic surfaces. *Appl. Environ. Microbiol.* **1979**, *37*, 480−486.
(15) Han, J.; Chen, L.; Duan, S. M.; Yang, Q. X.; Yang, M.; Gao, C.; Zhang, B. Y.; He, H.; Dong, X. P. Efficient and quick inactivation of SARS coronavirus and other microbes exposed to the surfaces of some metal catalysts. *Biomed. Environ. Sci.* **2005**, *18*, 176−180.
(16) Cagno, V.; Andreozzi, P.; D'Alicarnasso, M.; Jacob Silva, P.; Mueller, M.; Galloux, M.; Le Goffic, R.; Jones, S. T.; Vallino, M.; Hodek, J.; et al. Broad-spectrum non-toxic antiviral nanoparticles with a virucidal inhibition mechanism. *Nat. Mater.* **2018**, *17*, 195−203.
(17) Moridi, A.; Hassani-Gangaraj, S. M.; Guagliano, M.; Dao, M. Cold spray coating: review of material systems and future perspectives. *Surf. Eng.* **2014**, *30*, 369−395.
(18) Pelaz, B.; Jaber, S.; De Aberasturi, D. J.; Wulf, V.; Aida, T.; de la Fuente, J. M.; Feldmann, J.; Gaub, H. E.; Josephson, L.; Kagan, C. R.; Kotov, N. A.; Liz-Marzán, L. M.; Mattoussi, H.; Mulvaney, P.; Murray, C. B.; Rogach, A. L.; Weiss, P. S.; Willner, I.; Parak, W. J. The state of nanoparticle-based nanoscience and biotechnology: progress, promises, and challenges. *ACS Nano* **2012**, *6*, 8468−8483.
(19) Segets, D.; Lucas, J. M.; Klupp Taylor, R. N.; Scheele, M.; Zheng, H.; Alivisatos, A. P.; Peukert, W. Determination of the quantum dot band gap dependence on particle size from optical absorbance and transmission electron microscopy measurements. *ACS Nano* **2012**, *6*, 9021−9032.
(20) Yeshchenko, O. A.; Dmitruk, I. M.; Alexeenko, A. A.; Kotko, A. V.; Verdal, J.; Pinchuk, A. O. Size and temperature effects on the surface plasmon resonance in silver nanoparticles. *Plasmonics* **2012**, *7*, 685−694.
(21) Campbell, C. T.; Sellers, J. R. V. Anchored metal nanoparticles: Effects of support and size on their energy, sintering resistance and reactivity. *Royal Society of Chemistry (RSC)* **2013**, *162*, 9−30.
(22) Lin, N.; Verma, D.; Saini, N.; Arbi, R.; Munir, M.; Jovic, M.; Turak, A. Antiviral nanoparticles for sanitizing surfaces: a roadmap to self-sterilizing against COVID-19. *Nano Today* **2021**, *40*, 101267.
(23) Abulikemu, M.; Tabrizi, B. E. A.; Ghobadloo, S. M.; Mofarah, H. M.; Jabbour, G. E. Silver Nanoparticle-Decorated Personal Protective Equipment for Inhibiting Human Coronavirus Infectivity. *ACS Appl. Nano Mater.* **2022**, *5*, 309−317.
(24) Rogers, J. V.; Parkinson, C. V.; Choi, Y. W.; Speshock, J. L.; Hussain, S. M. A preliminary assessment of silver nanoparticle inhibition of monkeypox virus plaque formation. *Nanoscale Res. Lett.* **2008**, *3*, 129−133.
(25) Weiss, C.; Carriere, M.; Fusco, L.; Capua, I.; Regla-Nava, J. A.; Pasquali, M.; Scott, J. A.; Vitale, F.; Unal, M. A.; Mattevi, C.; et al. Toward nanotechnology-enabled approaches against the COVID-19 pandemic. *ACS Nano* **2020**, *14*, 6383−6406.
(26) Elechiguerra, J. L.; Burt, J. L.; Morones, J. R.; Camacho-Bragado, A.; Gao, X.; Lara, H. H.; Yacaman, M. J. Interaction of silver nanoparticles with HIV-1. *J. Nanobiotechnology* **2005**, *3*, 1−10.
(27) Tavakoli, A.; Hashemzadeh, M. S. Inhibition of herpes simplex virus type 1 by copper oxide nanoparticles. *J. Virol. Methods* **2020**, *275*, 113688.
(28) Hang, X.; Peng, H.; Song, H.; Qi, Z.; Miao, X.; Xu, W. Antiviral activity of cuprous oxide nanoparticles against Hepatitis C Virus in vitro. *J. Virol. Methods* **2015**, *222*, 150−157.
(29) Smith, J. L.; Tran, N.; Song, T.; Liang, D.; Qian, M. Robust bulk micro-nano hierarchical copper structures possessing exceptional bactericidal efficacy. *Biomaterials* **2022**, *280*, 121271.
(30) Das Jana, I.; Kumbhakar, P.; Banerjee, S.; Gowda, C. C.; Kedia, N.; Kuila, S. K.; Banerjee, S.; Das, N. C.; Das, A. K.; Manna, I.; et al. Copper Nanoparticle−Graphene Composite-Based Transparent Surface Coating with Antiviral Activity against Influenza Virus. *ACS Appl. Nano Mater.* **2021**, *4*, 352−362.
(31) Ermini, M. L.; Voliani, V. Antimicrobial Nano-Agents: The Copper Age. *ACS Nano* **2021**, *15*, 6008−6029.
(32) Behzadinasab, S.; Chin, A.; Hosseini, M.; Poon, L.; Ducker, W. A. A surface coating that rapidly inactivates SARS-CoV-2. *ACS Appl. Mater. Interfaces* **2020**, *12*, 34723−34727.
(33) Behzadinasab, A.; Williams, M. D.; Hosseini, M.; Poon, L. L. M.; Chin, A. W. H.; Falkinham, J. O.; Ducker, W. A. Transparent and Sprayable Surface Coatings that Kill Drug-Resistant Bacteria Within Minutes and Inactivate SARS-CoV-2 Virus. *ACS Appl. Mater. Interfaces* **2021**, *13* (46), 54706−54714.
(34) Hosseini, M.; Chin, A. W.; Behzadinasab, S.; Poon, L. L.; Ducker, W. A. Cupric oxide coating that rapidly reduces infection by SARS-CoV-2 via solids. *ACS Appl. Mater. Interfaces* **2021**, *13* (5), 5919−5928.
(35) El-Trass, A.; ElShamy, H.; El-Mehasseb, I.; El-Kemary, M. CuO nanoparticles: synthesis, characterization, optical properties and interaction with amino acids. *Appl. Surf. Sci.* **2012**, *258*, 2997−3001.
(36) Zhou, P.; Yang, X. L.; Wang, X. G.; Hu, B.; Zhang, L.; Zhang, W.; Si, H. R.; Zhu, Y.; Li, B.; Huang, C. L.; et al. A pneumonia outbreak associated with a new coronavirus of probable bat origin. *Nature* **2020**, *579*, 270−273.
(37) Booker, E. P.; Jabbour, G. E. Antiviral nanoparticle ligands identified with datamining and high-throughput virtual screening. *RSC Adv.* **2021**, *11* (37), 23136−23143.
(38) Naz, S.; Gul, A.; Zia, M. Toxicity of copper oxide nanoparticles: a review study. *IET Nanobiotechnol* **2020**, *14*, 1−13.
(39) Henson, T. E.; Navratilova, J.; Tennant, A. H.; Bradham, K. D.; Rogers, K. R.; Hughes, M. F. *In vitro* intestinal toxicity of copper oxide nanoparticles in rat and human cell models. *Nanotoxicology* **2019**, *13*, 795−811.
(40) Semisch, A.; Ohle, J.; Witt, B.; Hartwig, A. Cytotoxicity and genotoxicity of nano-and microparticulate copper oxide: role of solubility and intracellular bioavailability. *Part. Fibre Toxicol* **2014**, *11* (1), 1−16.
(41) *Material Safety Data Sheet Copper (II) Oxide*; SMARTLAB, 2018. http://smartlab.co.id/assets/pdf/MSDS_COPPER_(II)_OXIDE.pdf (accessed 2022-04-26).
(42) *Fact Sheet for Health Professionals*; National Institutes of Health Office of Dietary Supplements. https://ods.od.nih.gov/factsheets/Copper-HealthProfessional/ (accessed 2022-04-26).

https://doi.org/10.1021/acsabm.2c00229
ACS Appl. Bio Mater. XXXX, XXX, XXX−XXX